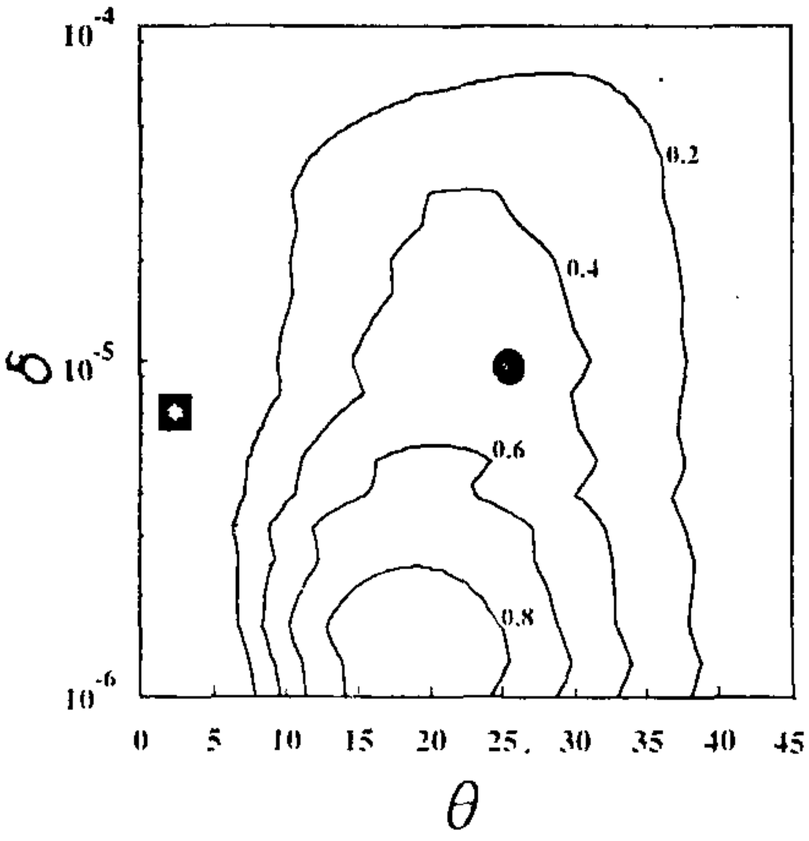

Figure 1. The contour plot of the enhancement in the neutrino detection rate $(R_2 - R_1)/R_1$ during a solar eclipse as a function of the neutrino mixing angle θ (in degrees) and the neutrino mass-difference parameter δ (in eV^2). The numbers 0.2–0.8 labelling the various curves are the values of $(R_2 - R_1)/R_1$. The dark square and circle correspond respectively to the central values of the 'small-angle' and 'large-angle' solutions of the solar neutrino problem.

there could be a sizeable increase in the flux of ν_e reaching the earth during the solar eclipse for some range of θ and δ. In particular for $\theta \approx 25°$ and $\delta \approx 10^{-5}\ eV^2$ which provides a solution[5] (the large angle solution) for the original solar neutrino puzzle, the increase is about 50% although for the small angle solution, the increase is only about 10%.

But the bad news is that the counting rate in the neutrino detectors is so small because of the notoriously tiny cross section σ for the interaction of the neutrinos with matter, that the enhancement in the counting rate during the few hours of the solar eclipse cannot be observed in any of the existing neutrino detectors which have a counting rate of utmost a few hundred per year and there is only a marginal possibility of its being seen even in the next generation of neutrino detectors[6] which will be ready soon, where the counting rate is expected to be of the order 10^4 per year. One must also add that the neutrino detectors are all huge and immovable, so in order to see the effect the detector must lie in the path of the eclipse. However, there are some positive factors. First the eclipse need not be a total one. Further, the effect can also be observed on the other side of the earth since the straightline connecting the sun and the moon during the eclipse cuts the surface of the earth at two points. In fact, on the far side of the earth the effect may be an enhanced one.

In any case, the aim of this communication is not to propose any experimental test of immediate relevance, but rather to focus general attention on the novelty of the phenomenon: the sun seen through ν_e radiation may shine brighter during the eclipse.

Finally one cannot avoid the temptation of speculating on the futuristic role of neutrino radiation since it is the most penetrating radiation known to man (except for gravitational radiation). The neutrino oscillation phenomenon is sensitively dependent on the density of matter traversed by the neutrinos, especially on its variation. Because of this, the possibility of using neutrino radiation from astrophysical sources for the tomography of the earth has already been speculated upon[7]. Similarly, monitoring of the solar neutrino radiation during the solar eclipse can lead to the tomography of the moon. Of course this has to wait until neutrino technology is mastered.

1. Sarma, K. V. L., *Int. J. Mod. Phys.*, 1995, **10**, 767–783.
2. Pal, P. B., *Int. J. Mod. Phys.*, 1992, **A7**, 5387–5459.
3. Hirata, K. S. *et al.*, *Phys. Rev. Lett.*, 1991, **66**, 9–12.
4. Kuo, T. K. and Pantaleone, J., *Rev. Mod. Phys.*, 1989, **61**, 937–979.
5. Hata, N. and Langacker, P., *Phys. Rev.*, 1994, **D50**, 632.
6. Pakvasa, S., in International Conference on Non-Accelerator Particle Physics (ed. Cowsik, R.), World Scientific, Singapore, 1995, pp. 188–201.
7. Learned, J. G. and Pakvasa, S., *Astroparticle Phys.*, 1995, **3**, 267–274.

ACKNOWLEDGEMENT. We thank Prof. N. D. Hari Dass for a helpful remark.

Received 21 December 1995; revised accepted 27 March 1996

A large conductance Ca^{2+}-activated K^+ channel in αT3-1 pituitary gonadotrophs

J. K. Tiwari, A. Adhikari and S. K. Sikdar

Molecular Biophysics Unit, Indian Institute of Science, Bangalore 560 012, India

The Ca^{2+}-activated K^+ channel in endocrine cells is responsible for membrane hyperpolarization and rhythmic firing of action potentials. The probability of opening of this channel is sensitive to intracellular-free Ca^{2+} concentration. In this study we have identified one such large conductance Ca^{2+}-activated K^+ channel in αT3-1 pituitary gonadotroph cell. This channel is ohmic with a unit conductance of 170 pS in symmetrical KCl (135 mM) and its current reverses near zero millivolts. When more than one channel is present in the patch membrane they open and close independent of each other, exhibiting no cooperativity between them as expected of a binomial distribution. The regulatory mechanism of this channel in modulating hormone secretion from αT3-1 gonadotroph cells is indicated.

BRAIN anterior pituitary gonadotrophs secrete luteinizing

hormone (LH) and follicle stimulating hormone (FSH) in response to the hypothalamic decapeptide, gonadotrophin releasing hormone (GnRH). The mechanism regulating pituitary hormone secretions has been suggested to involve changes in membrane potential and action potential frequency[1]. However, the electrophysiological events underlying this stimulus-secretion coupling in gonadotrophs are not well understood, primarily owing to the difficulty in identifying gonadotrophs in the heterogeneous population of pituitary cells. The immortalized αT3-1 gonadotroph cell line[2] which has receptors to GnRH and secretes α-FSH thus provides an interesting and suitable system for understanding the electrophysiological phenomena related to GnRH action.

Addition of GnRH to rat gonadotrophs causes rhythmic hyperpolarizations terminated by the firing of action potentials[3,4]. Of the different types of ionic channels present in the membrane of an excitable cell, the Ca^{2+}-activated K^+ channel provides an important link between intracellular Ca^{2+} and membrane potential changes. The intracellular Ca^{2+} concentration is known to rise in αT3-1 pituitary gonadotrophs following activation by GnRH[5,6]. Our findings on the large conductance Ca^{2+}-activated K^+ channel in αT3-1 pituitary gonadotrophs, using the patch-clamp technique[7] show that when two channels are present in the patch recording, they are functionally independent of each other.

The αT3-1 cell line (kindly provided by Dr Pamela Mellon, Univ. of California, San Diego, USA) was cultured in Dulbecco's Modified Eagle Medium (DMEM, Sigma) supplemented with 10% v/v foetal bovine serum (Gibco BRL) and antibiotics (1% v/v of Gibco BRL antibiotic–antimycotic solution). They were maintained in 25 cm^2 culture flasks (Nunc) at 5% CO_2 and 95% air humidified atmosphere at 37°C and cells were split on attaining 80% confluency. K^+ concentrations in Na^+-free internal and external solutions for the electrophysiological recording were the same (135 mM). The pipette solution contained (in mM) KCl 135, $CaCl_2 \cdot 2H_2O$ 2, Hepes 5, and glucose 10, pH 7.35, while the bath solution contained KCl 135, EGTA 1 and Hepes 5, pH 7.4. For the experiments to check cation specificity, the low KCl pipette solution contained (in mM) KCl 50, K-gluconate 90, $CaCl_2 \cdot 2H_2O$ 2, Hepes 5, pH 7.35, and the bath solution contained KCl 140, EGTA 1 and Hepes 5, pH 7.4. Recordings were done at 25 ± 2°C in an air-conditioned room.

In the inside-out configuration, Ca^{2+} concentrations in the intracellular face of the membrane, i.e. in the bath solution, were varied during the experiments. To achieve a desired level of free Ca^{2+}, the concentration of Ca^{2+} and EGTA to be added was obtained from the following equation[8]

$$Ca^{2+}_{total} = \frac{[Ca^{2+}]_i + K\{[Ca^{2+}]_i\,[EGTA] + [Ca^{2+}]_i^2\}}{1 + [Ca^{2+}]_i\,K}, \quad (1)$$

where Ca^{2+}_{total} is the concentration of Ca^{2+} to be added, $[Ca^{2+}]_i$ is the desired free calcium ion concentration in the Ca^{2+} EGTA buffer in bath, [EGTA] is total applied EGTA concentration in the bath solution and K is equilibrium constant of Ca^{2+} EGTA buffer ($K = 10^{7.130}$, pH 7.35 at 20°C).

Cells for recording were plated in 35 mm culture dishes (Tarsons, India) at low density and single isolated cells were used for recording after 24 h of plating. The recording was done using fire polished omega dot capillary micropipettes (INTRACEL Ltd, England), (pipette resistance 9–12 MΩ and seal resistance > 2 GΩ). Single channel currents were observed using the patch clamp technique[7] in inside-out configuration using the EPC-7 patch clamp amplifier (List-Medical, Germany). The recordings were stored in a DTR 1200 Digital tape-recorder (Bio-logic, France, frequency response DC to 48 kHz). The data was played back through a 1 kHz home-made Bessel filter and recorded into an IBM compatible PC-AT-286 computer interfaced with CED1401 AD converter (Cambridge Electronic Design, Cambridge, UK, sampling frequency 10 kHz). Analysis and fitting of the data were done using the PAT software (kindly provided by J. Dempster, Univ. of Strathclyde, Glasgow, Scotland).

Figure 1 shows single channel records at a fixed membrane voltage (+ 40 mV) in the inside-out configuration of the channel type being studied, but at three different $[Ca^{2+}]_i$ concentrations on the intracellular side. The indicated $[Ca^{2+}]_i$ concentrations were achieved by adding pre-determined aliquots of 10 mM $CaCl_2 \cdot 2H_2O$ stock solution directly to the bath medium (see equation (1)). The frequency of channel openings increased with increasing concentrations of $[Ca^{2+}]_i$. This confirms that these channels were sensitive to changes in $[Ca^{2+}]_i$ concentration. Similar results had previously been obtained in several other cell types[9–15]. The amplitude of the single channel current and the opening frequency of the channel was sensitive to changes in membrane potential, thus showing its potential dependence, but $[Ca^{2+}]_i$ *per se* did not influence single channel conductance.

Most of the recordings showed the existence of more than one active channel, indicating the possibility of their clustering. Clustering of up to 5 channels has been reported previously[16] and in such cases the gating mechanisms of individual channels have been found to be influenced[17]. We wished to establish that in recordings with more than one Ca^{2+}-activated K^+ channel in the patch membrane, the channels are functionally independent of one another.

It is experimentally possible to resolve the elementary currents from n number of channels in the patch membrane. In a multichannel recording an histogram of such events reveals a multimodal distribution with $n + 1$ peaks

(one for the closed state). The relative area under each peak can be interpreted as the probability of observing $1, 2, \ldots, n$ number of channels in the patch in open state. Figures 2 *a* and *b* show the amplitude distribution histograms for a typical one and two channel recording respectively. The histogram in Figure 2 *a* was fitted by a sum of two gaussian functions (see equation (2)), thereby indicating that the currents in the record originated from a single channel, which fluctuates between two conductance levels, i.e. open and closed. The sampled currents under the gaussian with mean value zero are identified as the currents under closed channel condition while the other gaussian represents currents from the open state. The mean value of the gaussian gives the estimate of the single channel current and the standard deviation of the gaussian represents the noise level of the recoding. The fractional area under each gaussian gives the probability p, of the channel being in the corresponding state. In the case of two channels in the patch membrane, amplitude distribution histograms were fitted with a sum of three gaussian functions as given in equation (2).

$$g = \sum_i \frac{A_i w}{\sqrt{2\pi\sigma_i^2}} \exp\left(\frac{-(I - I_{mi})^2}{2\sigma_i^2}\right), \qquad (2)$$

where A_i, I_{mi} and σ_i $(i = 1\text{–}3)$ are fractional area, mean current and standard deviation respectively of the corresponding gaussian, w is the bin width and I is the experimental current. The values of A_i, I_{mi} and σ_i are obtained by fitting the amplitude histograms with equation (2) using the iterative least squares curve fitting with the Levenberg–Marquardt search. The three gaussians can be interpreted to be an outcome of both channels closed, one channel open and both channels open conditions, because the mean value of the third gaussian is nearly twice that of the second gaussian. The probabilities that both channels are closed (p_0), one channel is open (p_1) and both channels are open (p_2) were estimated from the fractional area under the corresponding gaussians. Probability of single channel opening estimated from one channel patch as well as two channel patch was comparable under similar experimental conditions.

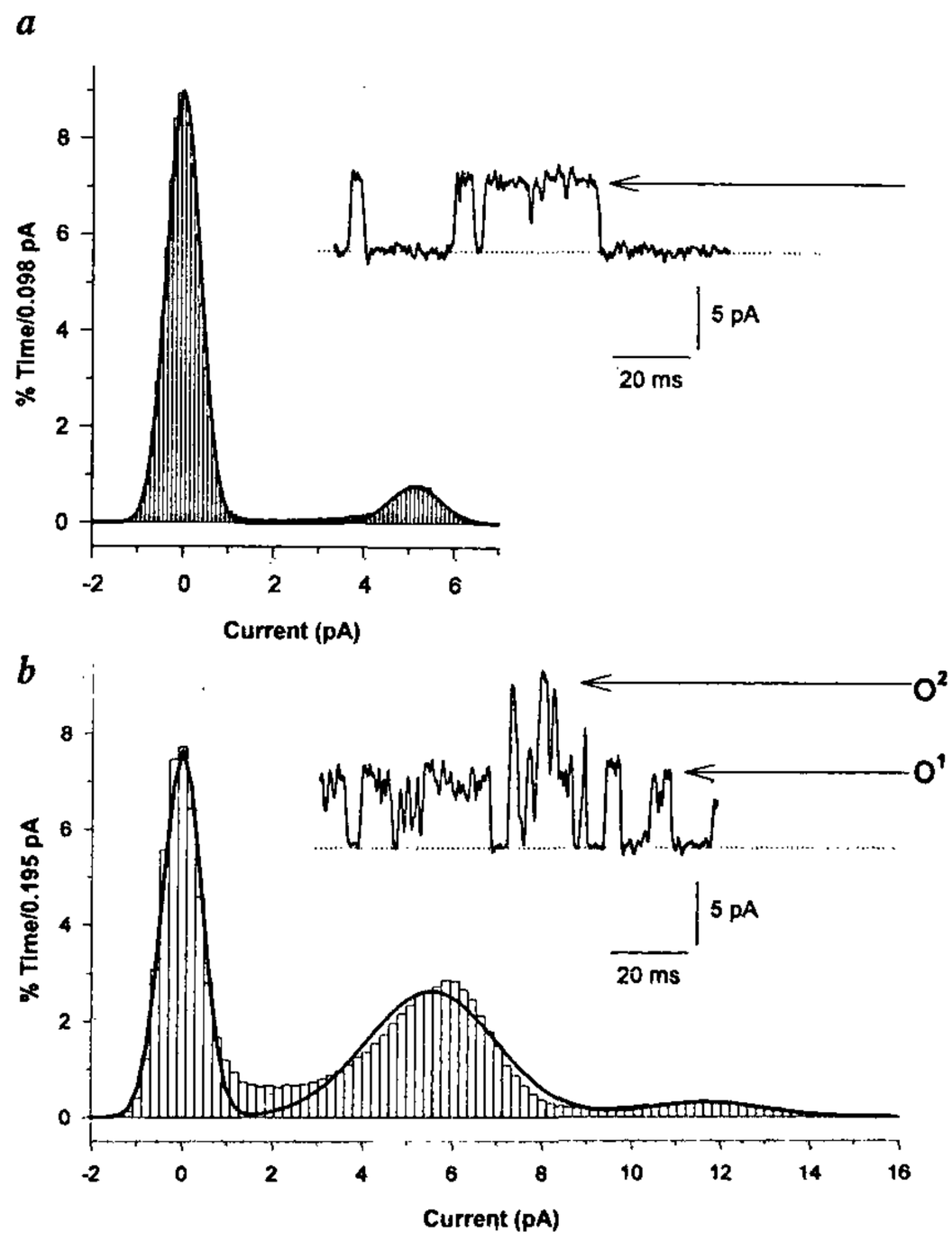

Figure 2 *a*, *b*. Amplitude histograms of inside-out Ca^{2+}-activated K^+ channel current recordings from a patch containing one (*a*) and two channels (*b*). $[Ca^{2+}]_i = 300$ nM and membrane potential = +30 mV. *a*, Amplitude histogram, solid line is the fitted gaussian (see text, equation (2)). Mean value of single channel current is 5.26 pA. Inset shows sample of single channel current trace from which the amplitude histogram was constructed. Dotted line indicates the closed state and arrow is the open state. The χ^2 value is 21.7 which is highly significant even at 99.5% confidence level with 123 degrees of freedom. *b*, Amplitude histogram constructed from a recording containing two channels. The histogram was fitted by a sum of three gaussians (see text, equation (2)), with mean single channel currents (determined from the gaussian fit) of 5.47 pA and 11.4 pA. Inset shows sample of current trace from which the histogram was constructed. O^1 is the current amplitude when one channel is conducting and O^2 is the current amplitude when both the channels are conducting. The χ^2 value is 20.6 which is significant at 99.5% confidence level with 92 degrees of freedom.

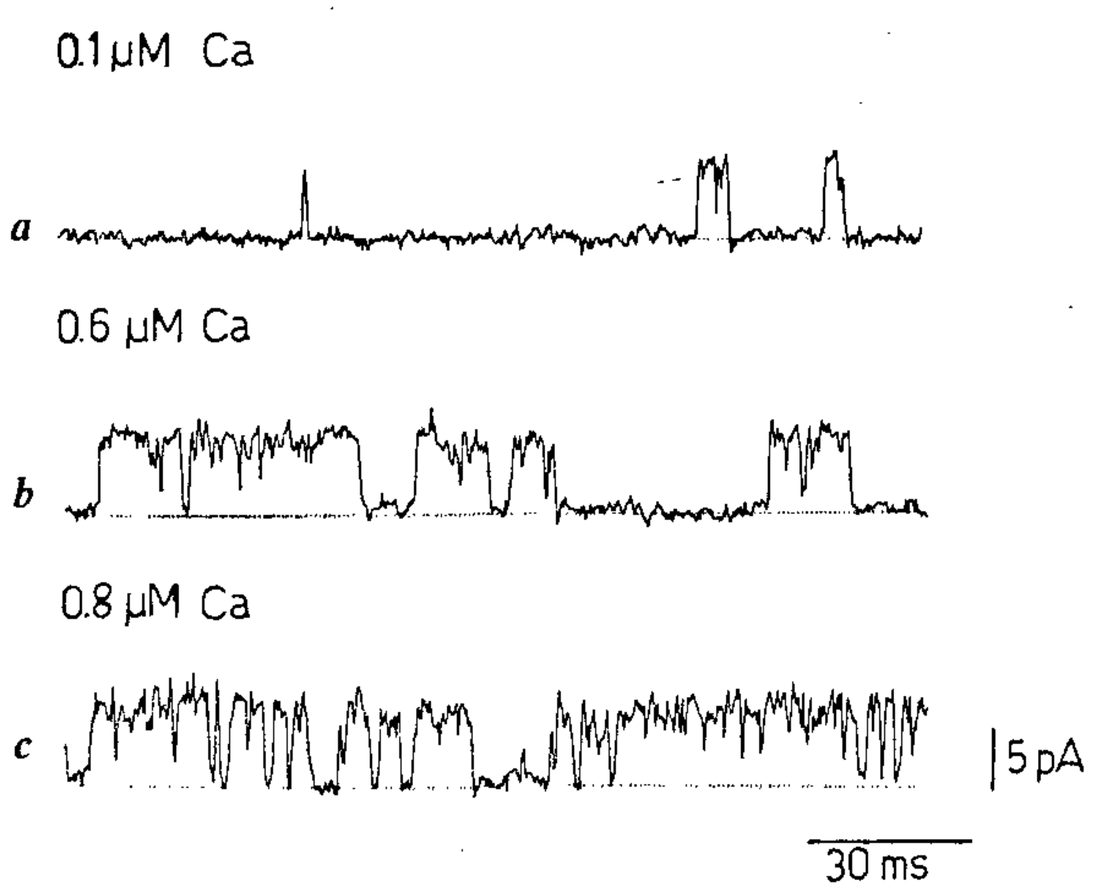

Figure 1. Activation of a single K^+ channel at different Ca^{2+} concentrations. The traces show stationary single inside-out K^+ channel current records from an αT3-1 cell at a transmembrane potential of 40 mV, in three different $[Ca^{2+}]_i$ concentrations. *a*, 100 nM Ca. *b*, 5 min following addition of $CaCl_2 \cdot 2H_2O$ to achieve 600 nM $[Ca^{2+}]_i$ concentration. *c*, 4 min after addition of $CaCl_2 \cdot 2H_2O$ to achieve 800 nM $[Ca^{2+}]_i$ concentration (bath volume = 2 ml).

For a collection of channel events having 2 values, viz. open and close, to be independent, the probability distribution is binomial[18]. Records containing more than one channel were used to establish if the channels open and close independent of each other by comparing the observed distribution of the current amplitudes to the estimated binomial distribution obtained from the following equation:

$$P_{(r)} = \frac{n!}{r!\,(n-r)!}\; p^r\,(1-p)^{n-r}. \qquad (3)$$

Figure 3 shows the experimental and estimated probabilities for a 2-channel recording at three different membrane potentials with fixed concentration of $[Ca^{2+}]_i$ (100 nM). No significant deviation was observed in any plots. The probability of opening was higher at + 60 mV as compared to + 50 and + 40 mV, which is expected of a channel showing voltage dependence (see legends to Figure 3). Similar results were obtained for a wide range of potentials and Ca^{2+} concentrations.

The current–voltage relationship for a typical Ca^{2+}-activated K^+ channel is shown in Figure 4. Figure 4 *a* shows single channel current traces at four different membrane potentials with equimolar KCl (135 mM) in pipette and bath. Figure 4 *b* demonstrates the dependence of single channel current amplitude on membrane potentials. The current reverses at – 3 mV with equimolar KCl in bath and pipette, which is close to potassium reversal potential. The cationic selectivity of the channel was tested by including 90 mM potassium gluconate + 50 KCl in pipette and 140 KCl in bath. Experiments similar to the one shown in Figure 4 *a* were conducted and the current reversed near 1 mV close to Nernst equilibrium potential for K^+ (see legend to Figure 4), the estimated reversal potential for chloride ion being + 26 mV. The Ca^{2+} sensitivity of the channel was confirmed by increasing the $[Ca^{2+}]_i$ from 0.1 to 0.6 µM. The specificity of the channel for K^+ was further judged from the change in the single channel current amplitude on changing the bath solution from 140 mM KCl to 70 mM KCl + 70 mM NaCl, while the pipette contained 140 mM KCl. The inside-out patch was held at 30 mV.

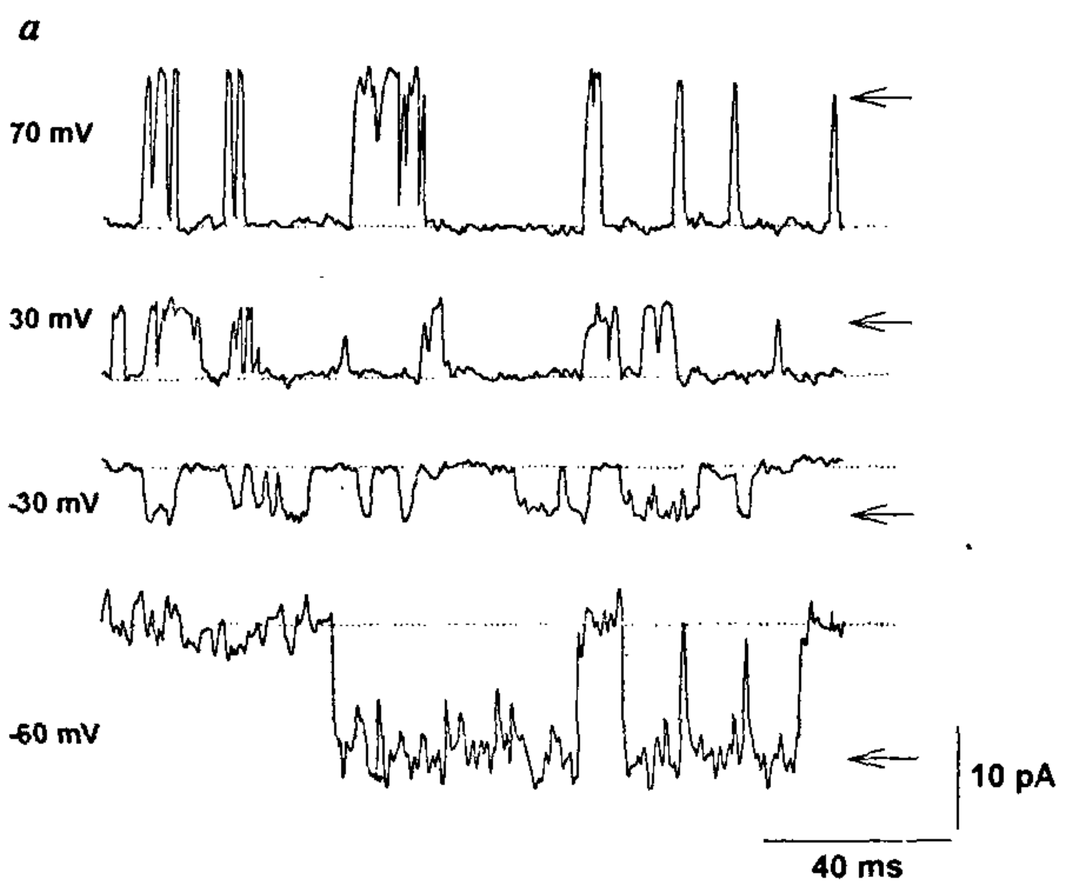

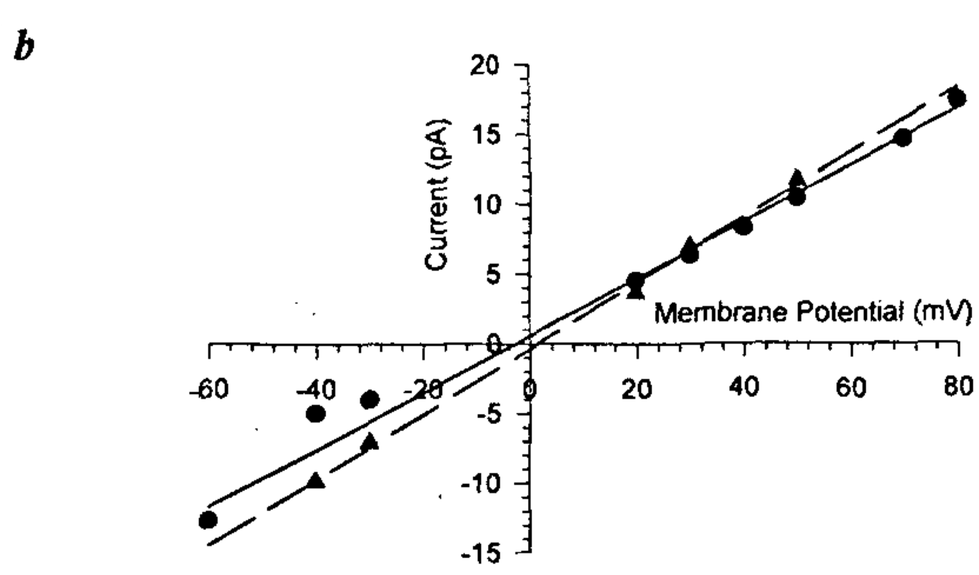

Figure 4 *a*, *b*. Single channel conductance plot. ***a***, Traces of single channel currents at various membrane potentials are indicated. Dotted line is the basal current level and arrow denotes the open channel current level. ***b***, Plot of single channel current amplitude vs membrane potential. The amplitude histogram was constructed for a 10 s recording, at each membrane potential. The current amplitudes were obtained by fitting the amplitude histogram with equation (2) (see text) and value of the parameter thus obtained is plotted. The solid circles are experimental points with symmetrical KCl (135 mM) in the bath and pipette solution and solid triangles represent the experimental points with low KCl in pipette (K-gluconate 90 mM + KCl 50 mM) and 140 mM KCl in bath. The lines are the best fitted first order linear regressions. The solid line is for symmetrical KCl in bath and pipette and dashed line is for low KCl in pipette. The conductance determined from slope of the solid line is 170 pS and correlation coefficient for the fit is 0.984. The dashed line is for the single channel currents in low KCl and the correlation coefficient for this is 0.993.

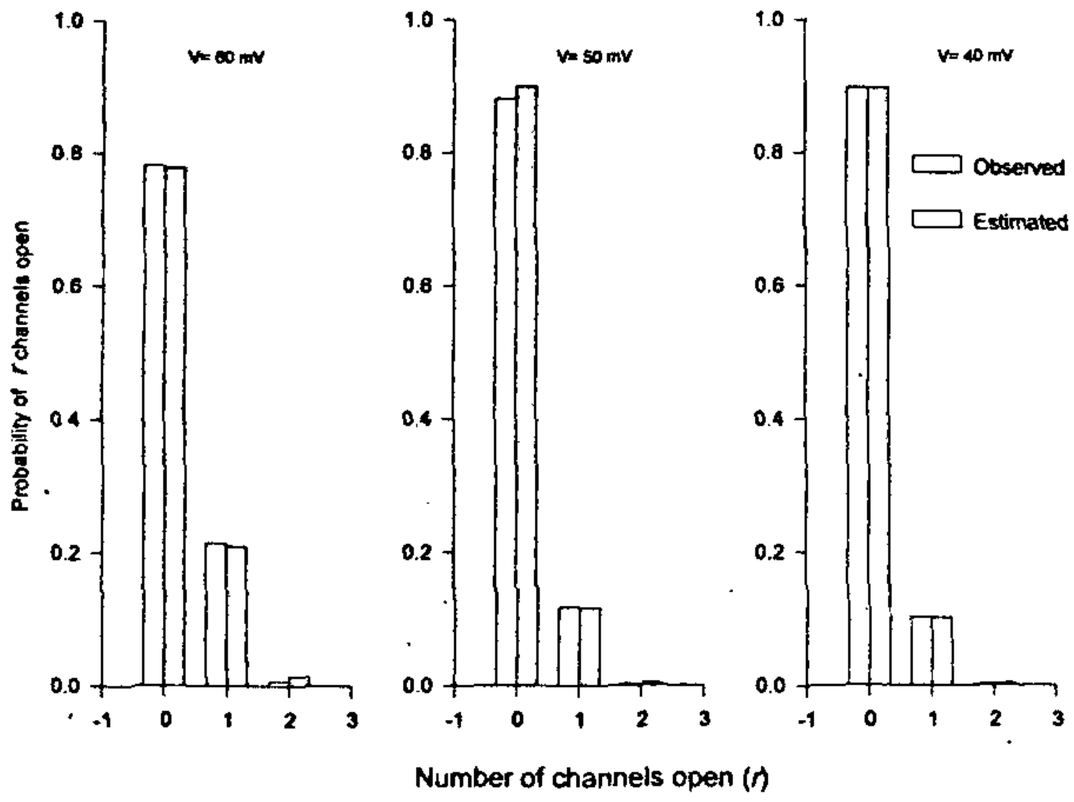

Figure 3. Binomial distribution of the probability of r channel opening in a two-channel inside-out patch. The empty bars are experimentally observed values obtained from the gaussian fits of amplitude histograms, and the shaded bars are theoretically estimated values of the same (see text, equation (3)). Probabilities of channel opening estimated from these records are 0.12, 0.062 and 0.053 at membrane potential V = 60, 50 and 40 mV respectively. Ca^{2+} concentration in bath = 100 nM. The maximum error between experimental and theoretical values is less than 2%, at the potentials indicated.

The single channel current amplitude reduced in 70 mM KCl + 70 mM NaCl solution as expected of a K^+ selective channel. Data in Figure 4 *b* were fitted by a straight line, suggesting that the channel is of ohmic type with single channel conductance of about 170 pS in symmetrical KCl. In the gluconate containing solution the single channel conductance was about 190 pS as calculated from the best fitted line (see Figure 4), which could be attributed to increased concentration of K^+ on either side of patch membrane.

The role of membrane hyperpolarization by Ca^{2+}-activated K^+ channels in hormone secretion has been described in a variety of endocrine cells[3,4]. Studies on Ca^{2+}-activated K^+ channels have shown that they are of different types. Based on studies using the patch-clamp technique, these channels have been broadly classified into large conductance channels (BK channels; conductance > 100 pS) and small conductance channels (SK channels). The conductance value obtained from I–V relationship shown in Figure 4 *b* suggests that the properties of the channel reported in this study may be a type of BK or maxi K(Ca) channel similar to those reported earlier[19,20]. We have also observed SK channels in our recording but the occurrence of these channels was less frequent in comparison to BK channels (data not shown).

Earlier studies have shown that Ca^{2+}-activated K^+ channels in a variety of cells are modulated by changes in free Ca^{2+} concentration at the intracellular membrane surface[13–15]. In this paper we show that Ca^{2+}-activated K^+ channels present in the αT3-1 gonadotroph cells are similarly modulated. Further, Ca^{2+} concentration affects the probability of opening of these channels but not their single channel conductance. Our observations are similar to those reported earlier in other systems[20]. Glasbey and Martin[17] have shown that when channels are clustered they mutually affect each other gating mechanism, but the results presented here suggest that when more than one channel is present in the patch, they operate independently of each others. With the dimension of pipette tip used in our experiments we have not encountered more than two channels in the patch membrane.

The observations presented in this study show how the Ca^{2+}-activated potassium channels could be involved in hormonal release. At rest the intracellular-free Ca^{2+} concentration in αT3-1 cells is between 50 and 100 nM (ref. 5). As shown in Figure 1, the probability of the channel being open would be low under these conditions. Following GnRH stimulation the Ca^{2+} concentration rises to about 600 nM (refs 5, 6), which would increase the open probability of the Ca^{2+}-activated K^+ channels which would lead to hyperpolarization of the membrane. Since these channels are also potential-dependent (Figure 3) these channels would also close, offsetting continuous hyperpolarization response by this self-feedback mechanism.

1. Ozawa, S. and Sand, O., *Physiol. Rev.*, 1986, **66**, 887–951.
2. Windle, J. J., Weiner, R. J. and Mellon, P. L., *Mol. Endocrinol.*, 1990, **4**, 597–603.
3. Tse, A. and Hille, B., *Science*, 1992, **255**, 462–464.
4. Kukuljan, M., Stojilkovic, S. S., Rojas, E. and Catt, K. J., *FEBS Lett.*, 1992, **301**, 19–22.
5. Anderson, L., Hoyland, J., Mason, W. T. and Eidne, K. A., *Mol. Cell. Endocrinol.*, 1992, **86**, 167–175.
6. Merelli, F., Stojikovic, S. S., Iida, T., Krsmanovic, L. Z., Zheng, L., Mellon, P. L. and Catt, K. J., *Endocrinology*, 1992, **131**, 925–932.
7. Hamill, O. P., Marty, A., Neher, E., Sakmann, B. and Sigworth, F. J., *Pflügers Archiv.*, 1981, **391**, 85–100.
8. Owen, J. D., *Biochim. Biophys. Acta*, 1976, **451**, 321–325.
9. Eckert, R. and Tillotson, D., *Science*, 1978, **200**, 437–439.
10. Atwater, I., Dawson, C. M., Ribalet, B. and Rojas, E., *J. Physiol. London*, 1979, **288**, 575–588.
11. Dunne, M. J., Findlay, I. and Petersen, O. H., *(Abst.) J. Physiol. London*, 1984, **354**, 44.
12. Findlay, I., Dunne, M. J. and Petersen, O. H., *J. Membr. Biol.*, 1985, **83**, 169–175.
13. Blatz, A. L. and Magleby, K. L., *Trends Neurosci.*, 1987, **10**, 463–467.
14. Latorre, R. A., Oberhauser, A., Labarca, P. and Alvarez, O., *Annu. Rev. Physiol.*, 1989, **51**, 385–399.
15. Latorre, R., in *Handbook of Membrane Channels* (ed. Peracchia, C.), Academic Press, New York, 1994, pp. 79–102.
16. Gola, M., Ducreux, C. and Changeux, H., *J. Physiol.*, 1990, **420**, 73–109.
17. Glasbey, C. A. and Martin, R. J., *J. Neurosci. Methods*, 1988, **24**, 183–287.
18. Colquhoun, D. and Hawkes, A. G., *Lectures on Biostatistics*, Oxford Univ Press, London, 1971.
19. Marty, A., *Nature*, 1981, **291**, 497–500.
20. Barrett, J. N., Magleby, K. L. and Pallotta, B. S., *J. Physiol.*, 1982, **331**, 211–230.

ACKNOWLEDGEMENTS. The studies were funded by grants from the Department of Biotechnology, Govt of India and partly by Erna and Victor Hasselblad Foundation (Sweden). We thank Dr Pamella Mellon (Univ. of California, San Diego, USA) for kindly providing us αT3-1 cells and Dr Anjali Karande (IISc, Bangalore, India) for help and suggestion in maintaining these cells. JKT is supported by a Senior Research Fellowship from CSIR, India.

Received 14 November 1995; revised accepted 9 April 1996